Diagnostic and Interventional Imaging 106 (2025) 53–59

Contents lists available at ScienceDirect

Diagnostic and Interventional Imaging

journal homepage: www.elsevier.com/locate/diii

Review

Photon-counting CT systems: A technical review of current clinical possibilities

Joël Greffier [a,1,*], Anaïs Viry [b,1], Antoine Robert [c], Mouad Khorsi [b], Salim Si-Mohamed [c,d]

[a] IMAGINE UR UM 103, Montpellier University, Department of Medical Imaging, Nîmes University Hospital, 30900 Nîmes, France
[b] Institute of Radiation Physics, Lausanne University Hospital and University of Lausanne, 1007 Lausanne, Switzerland
[c] University of Lyon, INSA-Lyon, University Claude Bernard Lyon 1, UJM-Saint Etienne, CNRS, Inserm, CREATIS UMR 5220, U1206, 69621 Villeurbanne, France
[d] Department of Radiology, Louis Pradel Hospital, Hospices Civils de Lyon, 69500 Bron, France

ARTICLE INFO

Keywords:
Computed tomography
Dual-energy CT
Image quality
Photon counting CT
Spectral photon counting CT

ABSTRACT

In recent years, computed tomography (CT) has undergone a number of developments to improve radiological care. The most recent major innovation has been the development of photon-counting detectors. By comparison with the energy-integrating detectors traditionally used in CT, these detectors offer better dose efficiency, eliminate electronic noise, improve spatial resolution and have intrinsic spectral sensitivity. These detectors also allow the energy of each photon to be counted, thus improving the sampling of the X-ray spectrum in multiple energy bins, to better distinguish between photoelectric and Compton attenuation coefficients, resulting in better spectral images and specific color K-edge images. The purpose of this article was to make the reader more familiar with the basic principles and techniques of new photon-counting CT systems equipped with photon-counting detectors and also to describe the currently available devices that could be used in clinical practice.

1. Introduction

In recent years, computed tomography (CT) has undergone a number of developments to improve medical care. These technological developments have been applied to acquisition (particularly by reducing rotation times, increasing the available tube voltage (kV) and tube current (mA) ranges, and using additional filtration) [1,2], detection (*e.g.*, reducing the size of z-axis detectors) [3], and reconstruction (*e.g.*, iterative or deep learning image reconstruction algorithms) [4-7]. These improvements have reduced the dose delivered to the patient while improving image quality by reducing image noise and/or improving spatial resolution [8-18].

Another major advance has been the development of dual-energy CT platforms [19-21]. These platforms are based on the acquisition or detection of two X-ray spectra at low and high energy, enabling the contribution of the photoelectric effect and the Compton effect to be assessed separately [19,22]. Spectral imaging can be used to generate different types of images and the additional information contained in these images facilitates the detection and characterization of lesions [19-21].

The latest major innovation has been the development of photon counting detectors (PCD) [19,23,24]. By comparison with the energy-integrating detectors (EIDs) traditionally used in CT, these detectors offer better dose efficiency, eliminate electronic noise, improve spatial resolution and have intrinsic spectral sensitivity [19,23,24]. These detectors also allow the energy of each photon to be counted, thus improving the sampling of the X-ray spectrum in multiple energy bins, to better distinguish between photoelectric and Compton attenuation coefficients, thus producing better spectral images and specific color K-edge images.

The purpose of this article was to make the reader more familiar with the basic principles and techniques of new photon-counting CT (PCCT) systems equipped with photon-counting detectors and also to describe the currently available devices that could be used in clinical practice.

2. Technical background

Spectral CT imaging is a generation of CT systems that uses the

Abbreviations: CT, Computed tomography; CdTe, Cadmium telluride; CZT, Cadmium zinc telluride; EID, Energy-integrating detectors; PCCT, Photon-counting CT; PCD, Photon-counting detectors; Si, Silicon.

* Corresponding author.
E-mail address: joel.greffier@chu-nimes.fr (J. Greffier).

[1] Both authors contributed equally to this work.

https://doi.org/10.1016/j.diii.2024.09.002
Received 12 August 2024; Accepted 3 September 2024
Available online 20 September 2024

energy-dependent information present in the images to explore new applications in clinical routine with material characterization. For more than two decades, dual-energy CT systems have been used to perform spectral imaging by distinguishing between low- and high-energy photons [19,25]. More recently, a newer generation of detectors, known as energy-resolving PCDs, has emerged to replace the conventional EIDs previously present in both conventional and dual-energy CT systems [26].

Energy-resolving PCDs offer significant advantages over conventional EIDs [27-29]. The main difference between EIDs and PCDs is the detection principle. EIDs use scintillators to convert X-ray photons into visible light, and then into electrical signals using photodiodes (Fig. 1a). EIDs collect and sum all the X-ray energy information without distinguishing between different energy levels. This loss of energy information degrades the spectral performance of dual-energy CT. On the opposite, PCDs use semiconductors to directly convert X-ray photons

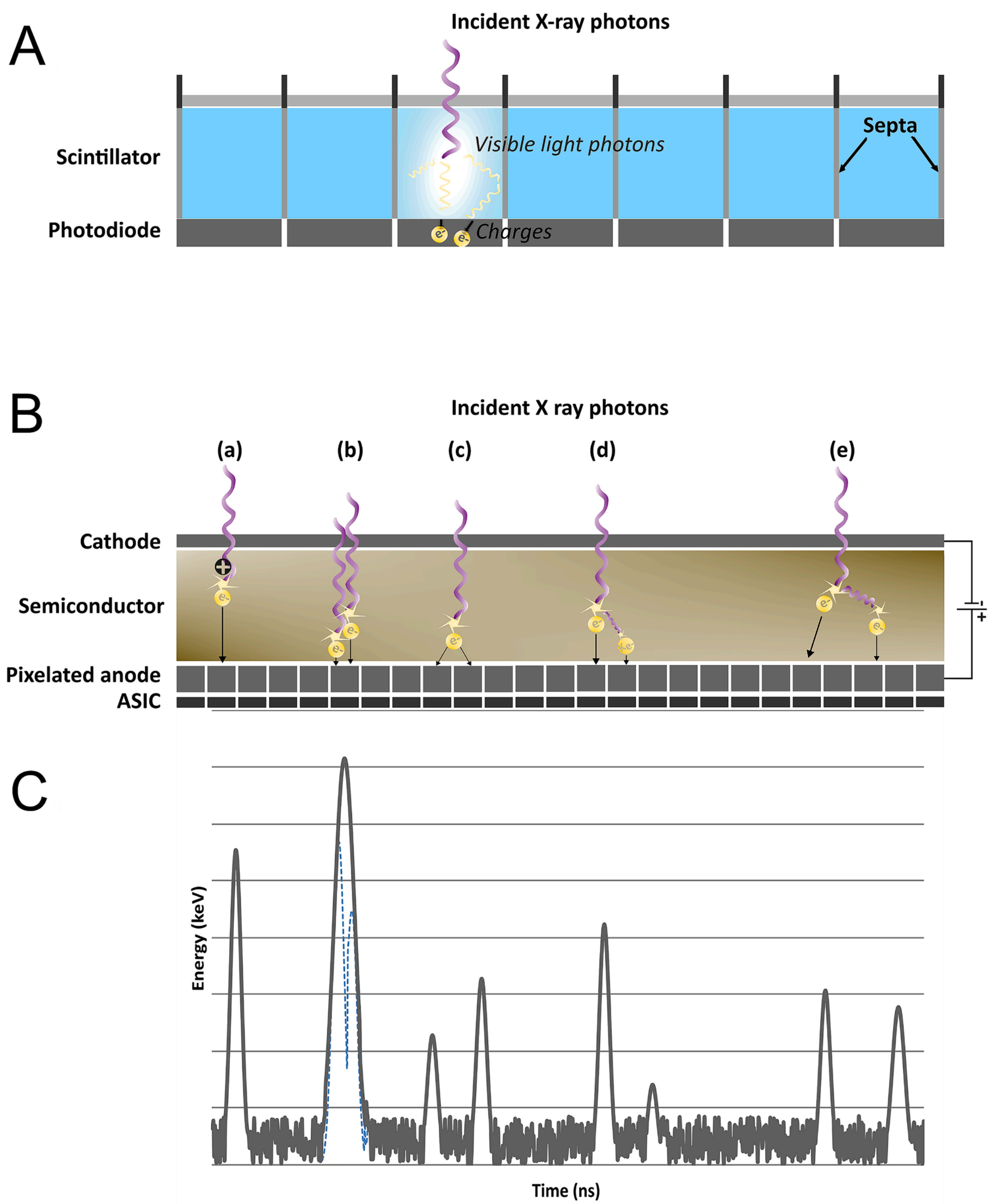

Fig. 1. Schematic representation of differences between energy-integrating detector (EID) and photon counting detector (PCD).
(**A**) EID measures the total energy deposited by incoming X-rays. A scintillator transforms X-ray photons to visible light that is detected by a photodiode. The use of septa creates dead space that limits the spatial resolution. (**B**) (a) PCD counts individual photons by directly converting photon energy to electric signal. (b) Pile-up effect occurs when multiple X-ray photons arrive at the detector within a short time, causing overlapping signals and compromising accurate energy measurement. (c) Charge sharing effect arises when the charge generated by a single X-ray photon is distributed between two detector elements, leading to reduced spatial and energy resolution. (d) k-escape is seen when a new charge cloud is generated by the Kα X-ray fluorescence of the sensor materials (CdTe or Si) and registered by a pixel as two separate events. (e) Compton scattering effects occur when any secondary photons produced in the semiconductor material is registered by the same pixel or an adjacent pixel as two separate events, yielding to a lower record of the real energy value (**C**) Graph shows the registered electric signal for each type of interaction

into electrical signals (Fig. 1b). PCDs are also called direct conversion detectors. A bias voltage is applied to the semiconductor sensors, an X-ray photon creates an electron/hole pair, resulting in a cloud of charges, that is directly processed by an application-specific integrated circuit to produce an electrical signal. This direct conversion enables PCDs to count each incoming photon individually and classify them based on their energy. Current PCCT systems exhibit variations in detector technology, energy resolution, spatial resolution and the number of energy thresholds available. Despite these differences, PCCT systems can precisely discriminate various materials of interest, while improving spatial resolution and decreasing noise [23,30-34].

2.1. Advantages of energy-resolving PCDs

2.1.1. Spatial resolution

The spatial resolution based on EIDs technology with CT systems is currently limited by two factors. The first one is the minimal size of detector elements using scintillators and the second one is the use of septa to avoid light diffusion within them, both of which create dead spaces. PCDs overcome both these limitations [23,24]. First, they are designed with pixel sizes at the isocenter ranging from 0.1 × 0.1 to 0.4 × 0.4 mm^2, smaller than those used in EIDs. Second, the direct conversion of X-ray photons into an electrical signal avoids the use of reflective septa. This is not only improves the spatial resolution, but also the radiation dose efficiency and geometric effectiveness.

2.1.2. Noise reduction and contrast improvement

Image noise arises from the statistical fluctuation of photons (the quantum noise) and electronic noise added by the electronic chain of EIDs [23,24]. X-ray tube filtration (inherent and, in some cases, additional) generally filters out low-energy photons below 20 keV. Therefore, the remaining low-energy signal detected by EIDs is due to electronic noise. In contrast, by implementing specific energy thresholds, PCDs can effectively filter out low-energy noise, resulting in a significant reduction in overall noise [23,24].

In addition, a current limitation of EID is the higher resulting electrical signal with high energy photons by comparison with low energy photons. This results in a loss of contrast because the photoelectric signal is dominated by low-energy photons. PCDs can register and count each individual incoming X-ray photon, accurately quantifying the X-ray signal and improving image contrast. Therefore, the higher contrast-to-noise ratio of PCDs can be used to reduce radiation dose in many applications of PCCT.

2.1.3. Material decomposition

Material decomposition relies on the energy dependence of the linear attenuation coefficient $\mu(\vec{x}, E)$ of materials in the diagnostic energy range (∼ 15–150 keV) proposed to model μ as the linear combination of energy-dependent and space-dependent function [35]:

$$\mu(\vec{x}, E) = \sum_{m=1}^{M} a_m(\vec{x}) f_m(E) \tag{1}$$

with $\vec{x}$ the 3D space position, E the energy, M the number of basis function, a_m the space-dependent functions and f_m the energy-dependent function. Knowing the energy functions f_m, the purpose of material decomposition is to obtain the volumes a_m.

For more than two decades, dual-energy CT has allowed the clinical use of spectral imaging. By measuring the X-ray attenuation in two different energy bins, material decomposition can be calculated using Eq. (1) with $M = 2$ to perform material decomposition. Two types of basis functions have been proposed for human tissue. The first approach consists of using the energy dependence of both the photoelectric interaction f_{Ph} and the total cross section for Compton scattering f_{Co}. Then, the volumes a_m describe the contributions of the photoelectric and Compton effects. As shown by Alvarez & Macovski, the function f_{Ph} can be approximated by $\frac{1}{E^3}$ and f_{Co} by the Klein-Nishina function [35]. Instead of using the photoelectric and Compton effect for the decomposition, the second approach uses the mass attenuation coefficient of two materials as energy-dependent basis functions. In this situation, the three-dimensional space-dependent functions a_m correspond to the local density of the materials. Water and calcium (bone) can be used as base materials, but most frequently iodine is injected, so water and iodine are the materials used. Dual-energy CT combined with material decomposition algorithm helps differentiate materials, improves tissue contrast and reduces artifacts (such as metal or beam hardening artifacts) compared to conventional CT [36-38]. Many clinical applications have been proposed using both material decomposition maps (*e.g.*, iodine maps or Z-effective) and virtual mono-energetic images [25].

Energy-resolving PCD could further advance spectral imaging a step further [30,39]. PCDs offer numerous advantages, one of which is to discriminate photons based on their energy with excellent resolution. This offers greater resolution of photoelectric and Compton contribution/absorption coefficients that will enhance the current known spectral capabilities such as virtual monochromatic images.

Another key advantage of PDCs is the ability to record photons in more than two energy bins, allowing for the inclusion of additional materials in the spectral decomposition. This enables the use of contrast agents based on their K-edge energies (*i.e.*, the binding energy between the K-shell and the nucleus). Indeed, at their K-absorption edges the atoms present a discontinuity in their attenuation spectra that can be used to discriminate them from other contributions to the global X-ray attenuation. This can be done by using Eq. (1) with $M = 3$ with the mass attenuation coefficient of the K-edge atom as additional energy-dependent function basis. Then, the local density of the atom can be obtained after the decomposition.

This approach, referred to as color K-edge imaging, allows the reconstruction of distinct images of both the contrast agent and the anatomy in a single CT acquisition [40,41]. In this sense, color K-edge is similar to the nuclear imaging twin modality of positron emission tomography/CT, in which low-resolution functional information from ^{18}F-fluorodeoxyglucose uptake is superimposed on high-resolution anatomical information. This opens up a completely new CT approach for functional, molecular or inflammation imaging and many other areas requiring exploration [42-47].

Fig. 2 shows a schematic representation of two-material decomposition and K-edge imaging on a numerical phantom. The phantom consists of a water cylinder with a gadolinium insert (K-edge energy of 50.2 keV) on the left and an insert of iodine on the right. The two-material decomposition with water and iodine as basis materials distinguishes the iodine from the water but the gadolinium appears in the iodine map. By adding the gadolinium as a third basie material, color K-edge imaging can also separate out iodine and gadolinium.

2.2. Technical limitations: charge sharing, pile-up, Compton scattering effects and energy resolution

Despite having many advantages by comparison with EID-CT, PCCT still suffers from some limitations that could mitigate performance [48]. First, the choice of semiconductor materials influences the energy resolution capabilities of PCDs, which can affect material differentiation, particularly when dealing with very similar energy levels [49]. Second, some issues like charge sharing, Compton scattering, k-escape and pile-up effects can introduce errors in data interpretation [48]. These effects are described in Fig. 1. The charge sharing effect occurs when a photon is counted by two adjacent pixels due to signal diffusion across adjacent detector elements. The simultaneous interactions are registered at lower energy, degrading both the spatial and energy resolutions. Similarly, Compton scattering effects occur when any secondary photons produced in the semiconductor material are registered by the same pixel or an adjacent pixel as two separate events, underestimating the

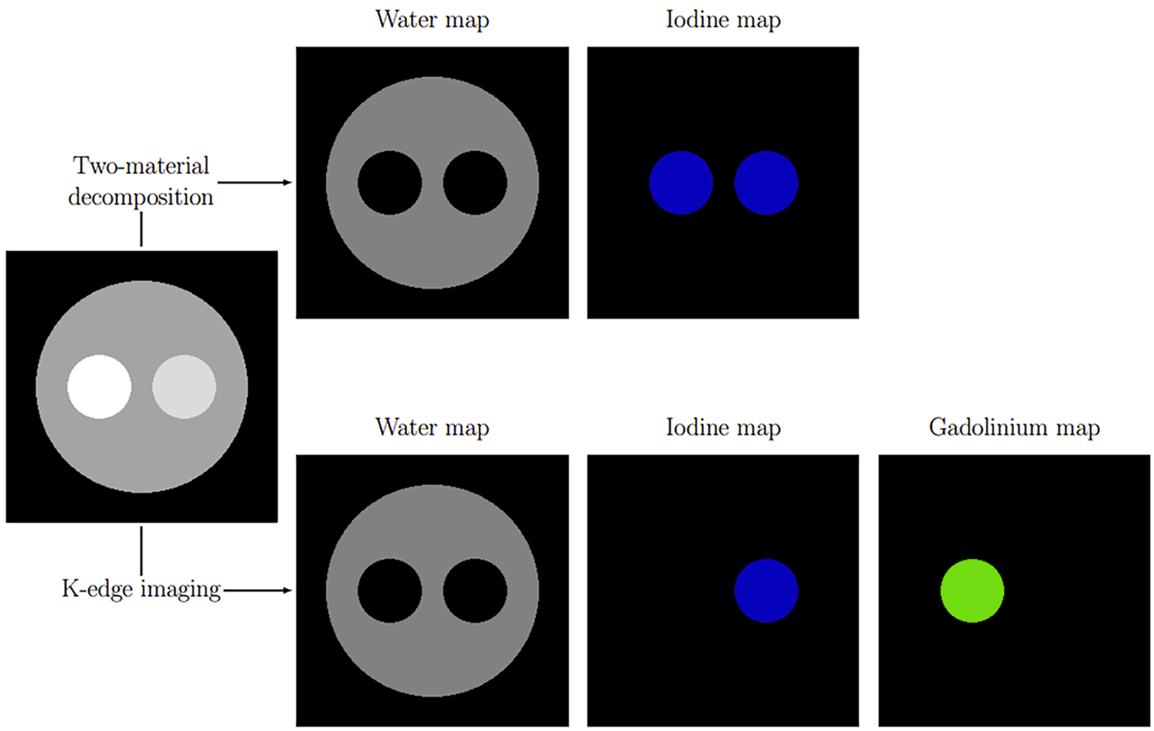

Fig. 2. Schematic representation of two-material decomposition and K-edge imaging on a numerical phantom. The phantom consists of a water cylinder with a gadolinium insert (K-edge energy of 50.2 keV) on the left and an insert of iodine on the right. Two-material decomposition with water and iodine as basis materials distinguishes the iodine from the water but the gadolinium appears in the iodine map. By adding the gadolinium as a third basis material, color K-edge imaging can also separate out iodine and gadolinium. Left: Conventional CT image of a numerical water phantom with one insert iodine (right) and one of gadolinium (left). Top row: Two-material decomposition using water and iodine as basis function. Bottom row: Color K-edge imaging done by adding the gadolinium as third material in the decomposition. For visualization, iodine map is colored in blue and gadolinium map in green.

real energy value. K-escape effect is seen when a new charge cloud is generated by the K X-ray fluorescence of the sensor materials and detected by a pixel as two separate events. The pile-up effect occurs when two consecutive photons are counted at the same time, yielding a loss of counts and an incorrect energy registration [50]. This effect is always present and depends on the count rates and dead time of the detector [51]. The distortion in the measured energy of individual events impacts the accuracy of energy assessment and material differentiation capabilities.

3. Technological differences between PCCT systems

3.1. Differences between PCDs

Currently, there are two main semiconductor materials used in clinical or pre-clinical PCCT systems: cadmium (zinc) telluride (CdTe or CZT) and silicon (Si). In comparison with CZT, CdTe sensor are easier to produce in large quantities and have better homogeneity and reproducibility. However, the presence of zinc in CZT detectors improves the resistivity in comparison with CdTe detectors.

The major difference between Si and CdTe/CZT sensors is the stopping power ratio. For the same material thickness, the absorption efficiency is around 5 % for Si and 90 % for the CdTe/CZT detectors [52] To obtain the same absorption efficiency between the two semiconductors, the thickness of Si should be equal to 55 mm [29]. As it is not feasible, the Si-semiconductor is mounted “edge on”, parallel to the incident X-ray direction. In comparison, the thickness of CZT semiconductor is around 2 mm and is mounted “face on”, perpendicular to the X-ray direction. The other difference between the two semiconductor materials comes from the different types of X-ray interaction into the semiconductor. With a high effective atomic number, CdTe or CZT have a higher probability of photo-electric absorption (84 %) than Si (28 %). X-ray interactions in Si are mainly Compton effect, that cause a loss of spatial resolution. The Si fluorescence peak have a characteristic energy of 1.74 keV that is filtrated as electronic noise. The detector quantum efficiency is also lower for Si-based PCD, that require a higher radiation dose than CdTe or CZT PCDs for a similar detection task [24]. On the other hand, CdTe or CZT have a high probability of k-fluorescence emission between 23 and 27 keV, which could deform the energy spectrum (particularly for low energies) and also degrade the spatial resolution. The advantages and limitations of both semiconductor materials are summarized in Table 1 [24,29,39].

Another semiconductor technology is currently under development with a Gallium-Arsenide sensor. However, no PCCT systems have yet used this technology. Their performance will not be described here and more information can be found in E. Hamann et al. paper [53].

Table 1
Comparison of characteristics between cadmium-based and silicon-based detectors.

Characteristic	Cadmium-based PCD (CdTe or CZT)	Sillicon-based PCD
Manufacturing complexity	Less complex	More complex
Thickness (orientation)	Face-on (1.4–2 mm)	Edge-on (30-60 mm)
Photo-electric effect / Compton effect	Photo-electric effect predominant	Compton effect predominant
k-fluorescence emission	Higher	Lower
Lowest energy bin	20–25 keV	5–10 keV
Energy resolution (FWHM)	5–10 keV	3–5 keV
Spatial resolution	Higher	Lower
Energy-resolving capabilities	Lower	Higher

CZT indicates cadmium-zinc telluride; CdTe indicates cadmium telluride; FWHM indicates full width at half maximum; PCD indicates photon-counting detectors.

3.2. Technological aspects of photon-counting CT platforms

Various CT manufacturers have developed PCCT systems and two PCCTs have been FDA approved (*i.e.*, one wide-bore for all applications and one small-bore for head imaging) [19,24]. The various systems developed differ in the choice of semi-conductor material used, the gantry types and the application domain (Table 2). All these choices have an impact on the performance of the PCCTs and the image quality, particularly in terms of spatial resolution and spectral performance. PCD detectors are also under development in cone-beam CT equipment, their performance will not be detailed here.

3.2.1. Siemens Healthineers

Siemens Healthineers were the first to obtain FDA approval (2021) for their wide-bore NAEOTOM Alpha CT system, which can be used for different application domains, including head, body, cardiac and extremity [23,24,26]. This PCCT has passed through several prototypes (CounT and Count Plus). It is a third generation dual-source system consisting of two X-ray tube/detector pairs dephased by 95° and equipped with CdTe semiconductor-based photon counting detectors. The detector array of the first detector covers a 50 cm field-of-view (FOV), while the second detected has an effective width of 36 cm, limiting its acquisition and reconstruction FOV to 36 cm for that one. CT acquisitions are usually carried out with a single X-ray tube, while two X-ray tubes are used for acquisitions requiring improved temporal resolution and/or high scan speeds (cardiac and high helical pitch scans with lowest rotation time of 0.25 s/rot and temporal resolution of 0.066 s). With this system, acquisitions can be made for different kVp (70, 90, 120, 140, Sn100 and Sn140 kVp) with 144 × 0.4 mm beam collimation in standard mode or 120 × 0.2 mm in high-resolution mode, resulting in effective detector element sizes at the isocenter of 0.30 × 0.30 mm^2 and 0.15 × 0.15 mm^2, respectively. For spectral images, materials can be decomposed using the data from four energy thresholds mixed to generate a low- and high-energy image in routine modes.

3.2.2. Samsung Healthcare

Samsung Healthcare were the second to obtain FDA approval (in 2022) for their small-bore OmniTom Portable PCD Head CT system, which can be used only for head CT acquisitions [54]. This portable system is composed by a single X-ray tube/detector pair equipped with CdTe semi-conductors. Acquisitions can be made for kV from 70 to 120 kVp with a beam collimation of 16 rows of 0.625 mm and 30-cm FOV. The detector size at the isocenter is 0.703 × 0.707 mm^2 for standard mode and 0.117 × 0.141 mm^2 or 0.351 × 0.423 mm^2 for high-resolution modes. For spectral images, materials can be decomposed using three energy bins.

3.2.3. MARS Bioimaging Limited

MARS Bioimaging Limited has developed a pre-clinical PCCT specifically designed for the upper-extremities [55]. This system consists of a single X-ray tube/detector pair equipped with CdZnTe semi-conductors. Unlike other CT systems, this system operates without a table, and the patient's upper extremity remains fixed while the pair (X-ray tube/detector) rotates. With this system, acquisitions can be performed at tube voltages ranging from 50 to 120 kVp, with a slice thickness of 0.09 mm, a 12.4 cm FOV, and a pixel size of 0.11 × 0.11 mm^2. For spectral images, materials can be decomposed using five energy bins in "charge summing" mode.

3.2.4. Canon Medical Systems

Canon Medical Systems has developed two PCCT versions. The first PCCT engineering prototype was developed on an Aquilion ONE ViSION CT platform [56] and the second is a clinical research PCCT (TSX-501R, Canon medical systems, Otawara, Japan) developed on an Aquilion PRECISION platform.

Both PCCT are single-source scanners equipped with CdZnTe semi-conductors. On both systems, acquisitions can be made at 120 kVp with a 50 cm FOV. For the first engineering prototype version, beam collimation is 16 × 0.62 mm in normal resolution mode (NR) and 48 × 0.21 mm in super-high-resolution mode (SHR) and 64 × 0.6 mm (NR) and 192 × 0.2 mm (SHR) on the Clinical Research PCCT version, respectively. The detector size at the isocenter is 0.2 × 0.2 mm^2 for both versions. For spectral images, materials can be decomposed using six energy bins for first version and five for the second.

3.2.5. Philips Healthcare

Philips Healthcare has developed an advanced research spectral PCCT prototype on the iCT platform, which could be used for all

Table 2
Main characteristics of current prototype, pre-clinical or clinical photon-counting CT (PCCT) systems suitable for clinical imaging.

Manufacturer	CT platforms	PCD materials	Geometry	Beam collimation	Field of view	Energy threshold	Current status
Siemens Healthineers	NAEOTOM Alpha	CdTe	Dual-source	STD: 144 × 0.4 mm HR: 120 × 0.2 mm	50 cm; 36 cm used for cardiac scanning; 36 cm for high helical pitch scanning	4 energy thresholds mixed to generate low and high energy bins in routine modes	FDA-cleared (September 2021)
Samsumg Healthcare	OmniTom Portable PCD Head CT	CdTe	Mono-source	16 × 0.625 mm	30 cm	3 available	FDA-cleared (March 2022)
MARS Bioimaging Limited	–	CdZnTe	Mono-source	14 mm	12.4 cm	5 in “charge summing mode”	Pre-clinical PCCT
Canon Medical Systems	Aquilion ONE ViSION CT	CdZnTe	Mono-source	STD: 16 × 0.62 mm HR: 48 × 0.21 mm	50 cm	6 available	Clinical prototype system
	Aquilion PRECISION	CdZnTe	Mono-source	STD: 64 × 0.6 mm HR: 192 × 0.2 mm	50 cm	5 available	Advanced clinical research PCCT
Philips Healthcare	iCT	CdZnTe	Mono-source	64 × 0.275 mm	50 cm	5 in standard mode; 5 in HR modes	Advanced research prototype system
GE Healthcare	LightSpeed Revolution CTRevolution Apex	Si	Mono-source	5 to 80 mm for CTRevolution Apex	50 cm	8 available	Advanced research prototype system

Parameters listed are based on the status of the manufacturer's development at time of publication and are expected to change in the near future.
Two CT platforms are designed with small bore gantry for head (Samsumg Healthcare) and for extremities (MARS Bioimaging limited system) imaging.
Cd indicates cadmium; FDA indicates Food and Drug Administration; HR indicates high-resolution mode; PCD indicates photon-counting detectors; Si indicates silicon; STD indicates standard; Te indicates telluride; Z indicates zinc.

application domains. The spectral PCCT is equipped with a single X-ray tube and a CdZnTe semiconductor detector array (2-mm thick). Acquisitions can be made at 80, 100, 120 or 140 kVp with a 50 cm FOV. The lowest available rotation time is 0.33 s/rot (from 0.33 to 1 s/rot) and the highest temporal resolution is 0.165 s. The beam collimation is 64 × 0.275 mm (z-coverage in the isocenter 17.5 mm) and the detector size at the isocenter is 274 × 274 μm^2 [32]. For spectral imaging, materials can be decomposed using five energy bins for both standard and high-resolution modes (*i.e.*, 512– or 1024–matrix sizes), with and without electrocardiogram gating [57-59]. This system has been used in preclinical and clinical research studies to evaluate novel K-edge contrast agents and to investigate the potential of spectral PCCT in a clinical setting.

3.2.6. GE Healthcare

To our knowledge, GE Healthcare is the only company that has developed three advanced research single-source prototypes equipped with deep silicon semiconductor detectors [19,24,29]. The first prototype was developed on a LightSpeed VCT platform, the second on a Revolution CT platform and the third on a Revolution Apex CT. With the third version of Si-PCCT prototype acquisitions are typically made at 120 kVp using axial and helical collimations of between 5 mm and 80 mm, with modules focally aligned in the x-direction to provide a 50-cm FOV. With this system the rotation time ranges from 0.234 to 1 s/rot, the matrix size is 1024 × 1024 pixels and the pixel size is 0.2 × 0.2 mm^2, with a sensitive volume at the isocenter of 0.2 × 0.2 × 0.4 mm (width × height × depth). The system is capable of using eight energy bins for spectral imaging tasks such as material decomposition.

4. Conclusion

The introduction of PCCT into clinical practice has opened a new era in medical imaging. The anticipated improvements in image quality are already being demonstrated in many applications, particularly those requiring better spatial resolution, contrast, and reduced radiation dose. In addition, this technology expands the capabilities of spectral CT for several applications that have not yet been fully exploited, especially with the development of color K-edge contrast agents. Overall, PCCT is expected to provide considerable benefits in the diagnosis, characterization, and staging of diseases, and to enable new approaches not previously possible with CT. However, PCCT systems are still scarce and open to technical developments that will facilitate the adoption of this technology.

Human rights

The authors declare that this article has been performed in accordance with the Declaration of Helsinki of the World Medical Association revised in 2013 for experiments involving humans.

Informed consent and patient details

The authors declare that this article does not contain any personal information that could lead to the identification of the patients.

Author contributions

All authors attest that they meet the current International Committee of Medical Journal Editors (ICMJE) criteria for Authorship.

Funding

This article did not receive any grant from funding agencies in the public, commercial, or not-for-profit sectors.

CRediT authorship contribution statement

Joël Greffier: Conceptualization, Methodology, Supervision, Validation, Writing – original draft, Writing – review & editing. **Anaïs Viry:** Conceptualization, Methodology, Supervision, Validation, Writing – original draft, Writing – review & editing. **Antoine Robert:** Conceptualization, Writing – original draft, Writing – review & editing. **Mouad Khorsi:** Conceptualization, Writing – original draft, Writing – review & editing. **Salim Si-Mohamed:** Conceptualization, Methodology, Supervision, Validation, Writing – original draft, Writing – review & editing.

Declaration of competing interest

The authors have no relevant conflict of interest to disclose in relation with this article.

Acknowledgements

We wish to thank Sarah Kabani, medical writer at the BESPIM, Nîmes University Hospital for her help in editing the manuscript. We also thank Kirsten Boedeker and Karim Haioun, (Canon Medical Systems), Philippe Coulon (Philips Healthcare), Håkan Grundin and Dominic Crotty (GE Healthcare), and Sebastian Faby (Siemens Healthineers) for reviewing and validating the sections related to their devices.

References

[1] Greffier J, Fitton I, Ngoc Ty CV, Frandon J, Beregi JP, Dabli D. Impact of tin filter on the image quality of ultra-low dose chest CT: a phantom study on three CT systems. Diagn Interv Imaging 2023;104:506–12.
[2] Greffier J, Pereira F, Hamard A, Addala T, Beregi JP, Frandon J. Effect of tin filter-based spectral shaping CT on image quality and radiation dose for routine use on ultralow-dose CT protocols: a phantom study. Diagn Interv Imaging 2020;101:373–81.
[3] Greffier J, Viry A, Durand Q, Hajdu SD, Frandon J, Beregi JP, et al. Brain image quality according to beam collimation width and image reconstruction algorithm: a phantom study. Phys Med 2023;108:102558.
[4] Geyer LL, Schoepf UJ, Meinel FG, Nance Jr JW, Bastarrika G, Leipsic JA, et al. State of the art: iterative CT reconstruction techniques. Radiology 2015;276:339–57.
[5] Greffier J, Frandon J, Larbi A, Beregi JP, Pereira F. CT iterative reconstruction algorithms: a task-based image quality assessment. Eur Radiol 2020;30:487–500.
[6] Willemink MJ, de Jong PA, Leiner T, de Heer LM, Nievelstein RA, Budde RP, et al. Iterative reconstruction techniques for computed tomography Part 1: technical principles. Eur Radiol 2013;23:1623–31.
[7] Willemink MJ, Noel PB. The evolution of image reconstruction for CT-from filtered back projection to artificial intelligence. Eur Radiol 2019;29:2185–95.
[8] Schwyzer M, Messerli M, Eberhard M, Skawran S, Martini K, Frauenfelder T. Impact of dose reduction and iterative reconstruction algorithm on the detectability of pulmonary nodules by artificial intelligence. Diagn Interv Imaging 2022;103:273–80.
[9] Akagi M, Nakamura Y, Higaki T, Narita K, Honda Y, Zhou J, et al. Deep learning reconstruction improves image quality of abdominal ultra-high-resolution CT. Eur Radiol 2019;29:6163–71.
[10] Greffier J, Boccalini S, Beregi JP, Vlassenbroek A, Vuillod A, Dupuis-Girod S, et al. CT dose optimization for the detection of pulmonary arteriovenous malformation (PAVM): a phantom study. Diagn Interv Imaging 2020;101:289–97.
[11] Greffier J, Macri F, Larbi A, Fernandez A, Khasanova E, Pereira F, et al. Dose reduction with iterative reconstruction: optimization of CT protocols in clinical practice. Diagn Interv Imaging 2015;96:477–86.
[12] Ichikawa Y, Kanii Y, Yamazaki A, Nagasawa N, Nagata M, Ishida M, et al. Deep learning image reconstruction for improvement of image quality of abdominal computed tomography: comparison with hybrid iterative reconstruction. Jpn J Radiol 2021;39:598–604.
[13] Jensen CT, Liu X, Tamm EP, Chandler AG, Sun J, Morani AC, et al. Image quality assessment of abdominal CT by use of new deep learning image reconstruction: initial experience. AJR Am J Roentgenol 2020;215:50–7.
[14] Boubaker F, Teixeira PAG, Hossu G, Douis N, Gillet P, Blum A, et al. In vivo depiction of cortical bone vascularization with ultra-high resolution-CT and deep learning algorithm reconstruction using osteoid osteoma as a model. Diagn Interv Imaging 2024;105:26–32.
[15] Nakamura Y, Narita K, Higaki T, Akagi M, Honda Y, Awai K. Diagnostic value of deep learning reconstruction for radiation dose reduction at abdominal ultra-high-resolution CT. Eur Radiol 2021;31:4700–9.
[16] Greffier J, Hamard A, Pereira F, Barrau C, Pasquier H, Beregi JP, et al. Image quality and dose reduction opportunity of deep learning image reconstruction algorithm for CT: a phantom study. Eur Radiol 2020;30:3951–9.
[17] Greffier J, Frandon J, Durand Q, Kammoun T, Loisy M, Beregi JP, et al. Contribution of an artificial intelligence deep-learning reconstruction algorithm for

dose optimization in lumbar spine CT examination: a phantom study. Diagn Interv Imaging 2023;104:76–83.
[18] Greffier J, Durand Q, Frandon J, Si-Mohamed S, Loisy M, de Oliveira F, et al. Improved image quality and dose reduction in abdominal CT with deep-learning reconstruction algorithm: a phantom study. Eur Radiol 2023;33:699–710.
[19] Greffier J, Villani N, Defez D, Dabli D, Si-Mohamed S. Spectral CT imaging: technical principles of dual-energy CT and multi-energy photon-counting CT. Diagn Interv Imaging 2023;104:167–77.
[20] Agostini A, Borgheresi A, Mari A, Floridi C, Bruno F, Carotti M, et al. Dual-energy CT: theoretical principles and clinical applications. Radiol Med 2019;124:1281–95.
[21] McCollough CH, Leng S, Yu L, Fletcher JG. Dual- and multi-energy CT: principles, technical approaches, and clinical applications. Radiology 2015;276:637–53.
[22] Greffier J, Si-Mohamed S, Dabli D, de Forges H, Hamard A, Douek P, et al. Performance of four dual-energy CT platforms for abdominal imaging: a task-based image quality assessment based on phantom data. Eur Radiol 2021;31:5324–34.
[23] Leng S, Bruesewitz M, Tao S, Rajendran K, Halaweish AF, Campeau NG, et al. Photon-counting detector CT: system design and clinical applications of an emerging technology. Radiographics 2019;39:729–43.
[24] Toia GV, Mileto A, Borhani AA, Chen GH, Ren L, Uyeda JW, Marin D. Approaches, advantages, and challenges to photon counting detector and multi-energy CT. Abdom Radiol 2024;49:3251–60.
[25] McCollough CH, Boedeker K, Cody D, Duan X, Flohr T, Halliburton SS, et al. Principles and applications of multienergy CT: report of AAPM Task Group 291. Med Phys 2020;47:e881–912.
[26] Rajendran K, Petersilka M, Henning A, Shanblatt ER, Schmidt B, Flohr TG, et al. First clinical photon-counting detector CT system: technical evaluation. Radiology 2022;303:130–8.
[27] Wehrse E, Klein L, Rotkopf LT, Wagner WL, Uhrig M, Heussel CP, et al. Photon-counting detectors in computed tomography: from quantum physics to clinical practice. Radiologe 2021;61:1–10.
[28] Roessl E, Brendel B, Engel KJ, Schlomka JP, Thran A, Proksa R. Sensitivity of photon-counting based K-edge imaging in X-ray computed tomography. IEEE Trans Med Imaging 2011;30:1678–90.
[29] Danielsson M, Persson M, Sjolin M. Photon-counting x-ray detectors for CT. Phys Med Biol 2021;66:03TR01.
[30] Willemink MJ, Persson M, Pourmorteza A, Pelc NJ, Fleischmann D. Photon-counting CT: technical principles and clinical prospects. Radiology 2018;289: 293–312.
[31] Lennartz S, Schoenbeck D, Kröger JR, Borggrefe J, Henning Niehoff J. Photon-counting CT material decomposition: initial experience in assessing adrenal adenoma. Radiology 2023;306:202–4.
[32] Si-Mohamed SA, Boccalini S, Villien M, Yagil Y, Erhard K, Boussel L, et al. First experience with a whole-body spectral photon-counting CT clinical prototype. Invest Radiol 2023;58:459–71.
[33] Douek PC, Boccalini S, Oei EHG, Cormode DP, Pourmorteza A, Boussel L, et al. Clinical applications of photon-counting CT: a review of pioneer studies and a glimpse into the future. Radiology 2023;309:e222432.
[34] Si-Mohamed SA, Miailhes J, Rodesch PA, Boccalini S, Lacombe H, Leitman V, et al. Spectral photon-counting CT technology in chest imaging. J Clin Med 2021;10: 5757.
[35] Alvarez RE, Macovski A. Energy-selective reconstructions in X-ray computerized tomography. Phys Med Biol 1976;21:733–44.
[36] Garnett R. A comprehensive review of dual-energy and multi-spectral computed tomography. Clin Imaging 2020;67:160–9.
[37] Omoumi P, Becce F, Racine D, Ott JG, Andreisek G, Verdun FR. Dual-energy CT: basic principles, technical approaches, and applications in musculoskeletal imaging (Part 1). Semin Musculoskelet Radiol 2015;19:431–7.
[38] Machida H, Tanaka I, Fukui R, Shen Y, Ishikawa T, Tate E, Ueno E. Dual-energy spectral CT: various clinical vascular applications. Radiographics 2016;36:1215. -132.
[39] Dane B, Froemming A, Schwartz FR, Toshav A, Ramirez-Giraldo JC, Ananthakrishnan L. Photon counting CT clinical adoption, integration, and workflow. Abdom Radiol 2024. https://doi.org/10.1007/s00261-024-04503-5.
[40] Nizovtseva IG, Galenko PK. Travelling-wave amplitudes as solutions of the phase-field crystal equation. Philos Trans A Math Phys Eng Sci 2018;376:20170202.
[41] Cuau L, Akl P, Gautheron A, Houmeau A, Chaput F, Yaromina A, et al. Surface modification effect on contrast agent efficiency for X-ray based spectral photon-counting scanner/luminescence imaging: from fundamental study to in vivo proof of concept. Nanoscale 2024;16:2931–44.
[42] Si-Mohamed SA, Sigovan M, Hsu JC, Tatard-Leitman V, Chalabreysse L, Naha PC, et al. In vivo molecular K-edge imaging of atherosclerotic plaque using photon-counting CT. Radiology 2021;300:98–107.
[43] Boccalini S, Mayard C, Lacombe H, Villien M, Si-Mohamed S, Delahaye F, et al. Ultra-high-resolution and K-edge imaging of prosthetic heart valves with spectral photon-counting CT: a phantom study. Invest Radiol 2024;59:589–98.
[44] Cosset B, Sigovan M, Boccalini S, Farhat F, Douek P, Boussel L, et al. Bicolor K-edge spectral photon-counting CT imaging for the diagnosis of thoracic endoleaks: a dynamic phantom study. Diagn Interv Imaging 2023;104:235–42.
[45] Si-Mohamed S, Cormode DP, Bar-Ness D, Sigovan M, Naha PC, Langlois JB, et al. Evaluation of spectral photon counting computed tomography K-edge imaging for determination of gold nanoparticle biodistribution in vivo. Nanoscale 2017;9: 18246–57.
[46] Si-Mohamed S, Tatard-Leitman V, Laugerette A, Sigovan M, Pfeiffer D, Rummeny EJ, et al. Spectral photon-counting computed tomography: in-vivo single-acquisition multi-phase liver imaging with a dual contrast agent protocol. Sci Rep 2019;9:8458.
[47] Si-Mohamed S, Thivolet A, Bonnot PE, Bar-Ness D, Kepenekian V, Cormode DP, et al. Improved peritoneal cavity and abdominal organ imaging using a biphasic contrast agent protocol and spectral photon counting computed tomography K-edge imaging. Invest Radiol 2018;53:629–39.
[48] Si-Mohamed S, Bar-Ness D, Sigovan M, Cormode DP, Coulon P, Coche E, et al. Review of an initial experience with an experimental spectral photon-counting computed tomography system. Nucl Instrum Methods Phys Res 2017;873:27–35.
[49] Persson M, Wang A, Pelc NJ. Detective quantum efficiency of photon-counting CdTe and Si detectors for computed tomography: a simulation study. J Med Imaging 2020;7:043501.
[50] Wang AS, Harrison D, Lobastov V, Tkaczyk JE. Pulse pileup statistics for energy discriminating photon counting x-ray detectors. Med Phys 2011;38:4265–75.
[51] Hsieh SS, Rajbhandary PL, Pelc NJ. Spectral resolution and high-flux capability tradeoffs in CdTe detectors for clinical CT. Med Phys 2018;45:1433–43.
[52] Ballabriga R, Alozy J, Campbell M, Frojdh E, Heijne EHM, Koenig T, et al. Review of hybrid pixel detector readout ASICs for spectroscopic X-ray imaging. J Instrum 2016;11:P01007.
[53] Hamann E, Koenig T, Zuber M, Cecilia A, Tyazhev A, Tolbanov O, et al. Performance of a Medipix3RX spectroscopic pixel detector with a high resistivity gallium arsenide sensor. IEEE Trans Med Imaging 2015;34:707–15.
[54] Park SJ, Park J, Kim D, Lee D, Lee CL, Bechwati I, et al. The first mobile photon-counting detector CT: the human images and technical performance study. Phys Med Biol 2023;68:9.
[55] Gallego Manzano L, Monnin P, Sayous Y, Becce F, Damet J, Viry A. Clinical commissioning of the first point-of-care spectral photon-counting CT for the upper extremities. Med Phys 2023;50:2844–59.
[56] Zhan X, Zhang R, Niu X, Hein I, Budden B, Wu S, et al. Comprehensive evaluations of a prototype full field-of-view photon counting CT system through phantom studies. Phys Med Biol 2023;68:17.
[57] Si-Mohamed SA, Boccalini S, Lacombe H, Diaw A, Varasteh M, Rodesch PA, et al. Coronary CT angiography with photon-counting CT: first-in-human results. Radiology 2022;303:303–13.
[58] van der Werf NR, Si-Mohamed S, Rodesch PA, van Hamersvelt RW, Greuter MJW, Boccalini S, et al. Coronary calcium scoring potential of large field-of-view spectral photon-counting CT: a phantom study. Eur Radiol 2022;32:152–62.
[59] Greffier J, Si-Mohamed SA, Lacombe H, Labour J, Djabli D, Boccalini S, et al. Virtual monochromatic images for coronary artery imaging with a spectral photon-counting CT in comparison to dual-layer CT systems: a phantom and a preliminary human study. Eur Radiol 2023;33:5476–88.